RELATIONSHIP BETWEEN THE AVERAGE S-WAVE VELOCITY AND SITE AMPLIFICATION RATIO USING K-NET RECORDS

Isamu TAMURA[1], Fumio YAMAZAKI[2], Khosrow T. SHABESTARI[3]

ABSTRACT

In order to evaluate seismic vulnerability of a region, accurate estimation of site amplification characteristics of strong ground motion is necessary. In this study, the average shear wave velocity (*AVS*) of surface layers is highlighted as an indicator predicting the site amplification. The attenuation relations developed for Japanese strong motion data recorded by K-NET were used and the station coefficient representing the site effect was compared with the *AVS* of each site. Calculating the *AVS* in 1 meter pitch from the surface, the depth showing the highest correlation between the station coefficient and *AVS* was obtained for PGA, PGV and response spectrum. The results indicate that the depth depends on the strong motion index and the period of the response spectrum. The obtained relationships can be used for the estimation of site amplification characteristics at the location of borehole data.

Introduction

Estimation of strong ground motion distribution is necessary in order to evaluate seismic vulnerability of a region (Yamazaki et al. 1998). In order to apply the estimation into a disaster information system, a method that enables the estimation from recorded data is desirable. A common method to estimate the ground motion is to develop attenuation relationships for strong ground motion indices as a function of the magnitude, the shortest distance from the fault rupture, the depth, and the site-specific term (station coefficient). Shabestari and Yamazaki (2000) developed attenuation relationships for the strong ground motion indices and response spectra from the K-NET records. In this study, the site amplification characteristics represented by the station coefficients in these attenuation models are employed.

Recently, several studies on the estimation of the site amplification using recorded data have been conducted. Matsuoka and Midorikawa (1995) proposed a method to estimate the site amplification of each topographical class in Digital National Land Information (DNLI) of Japan from the average S-wave velocity (the *AVS*). Fukuwa et al. (1998) proposed a method to estimate the amplification ratios of the peak ground acceleration (PGA) and the peak ground velocity (PGV) based on the DNLI using the results of earthquake response analyses for Aichi-Nagoya region. Yamazaki et al. (2000) investigated the relationship between the station coefficients obtained from the attenuation relations for JMA-87type-accelerometer records and the geomorphological land classification in the DNLI and proposed a method to estimate the site amplification ratios of PGA and PGV for all over Japan.

[1] Department of Civil Engineering, The University of Tokyo, Japan
[2] Institute of Industrial Science, the University of Tokyo, Japan
[3] Earthquake Disaster Mitigation Research Center, The Institute of Physical and Chemical Research, Japan

In these studies, the amplification ratio is defined for topographic or geomorphological categories in the DNLI. But in order to apply the estimation into a region where seismometers are placed in high density, such site classification may not be detailed enough to represent the site response characteristics. In this study, a method to estimate the site amplification from the *AVS* is proposed in order to obtain more accurate estimation.

Attenuation Relationships and Site Amplification

Shabestari and Yamazaki (2000) developed the attenuation relationships for the PGA and PGV and response spectra by using K-NET records, consisting of 6017 three-component sets from 94 events with the JMA magnitude equal or greater than 5.0. These data were recorded at 823 free field sites in Japan (Fig. 1) from May 1, 1996 to December 31, 1998. Distribution of the PGA with JMA magnitude for the current data set is shown in Fig. 2.

The attenuation model for the PGA or PGV is given by

$$\log_{10} y = b_0 + b_1 M + b_2 r - \log_{10} r + b_4 h + c_i \quad (1)$$

and the model for the response spectra is given by

$$\log_{10} y(T) = b_0(T) + b_1(T) M + b_2(T) r - \log_{10} r + b_4(T) h + c_i(T) \quad (2)$$

in which y is the strong ground motion index or the response spectra, M is the JMA magnitude, r is the shortest distance from the fault rupture, h is the depth, c_i is the coefficient representing local site effect of the ith station, and b's are the coefficients to be determined. In the model for the response spectra, y and b's are defined as functions of period. Note that the mean value of all the station coefficients is zero. In this study, the site amplification characteristics are represented by the station coefficients. Thus the site amplification compared to the average site is defined as 10^{ci}.

Average S-wave Velocity and Amplification Theory

There are two definitions in calculating the *AVS*, $AVS_T(d)$ derived from the total running time of the S-wave in each layer, and $AVS_L(d)$ derived from the mean value of the velocity weighted by the thickness of each layer. The definitions are given by the equations (3) and (4) with d being the depth.

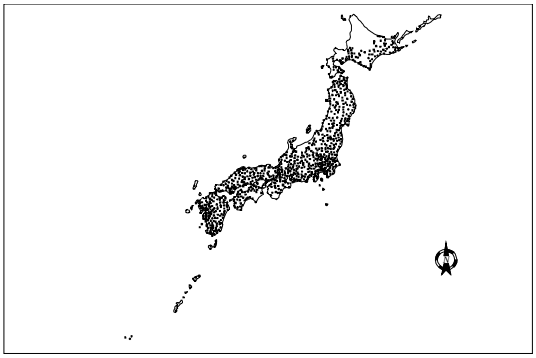

Figure 1 Location of the K-NET stations

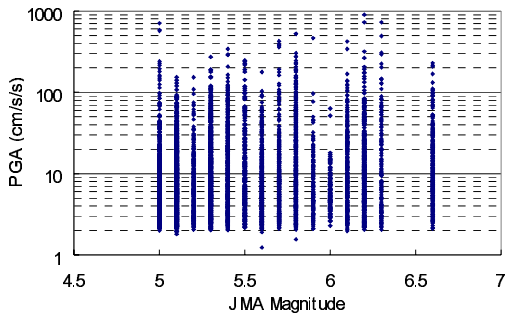

Figure 2 Distribution of the K-NET data used on the PGA and JMA magnitude plane

$$AVS_T(d) = \frac{d}{\sum h_i / V_{si}} \qquad (3)$$

$$AVS_L(d) = \frac{\sum V_{si} h_i}{d} \qquad (4)$$

The comparison between the two definitions is shown in Fig. 3, in which the value of $AVS_T(d)$ is constantly smaller than that of $AVS_L(d)$.

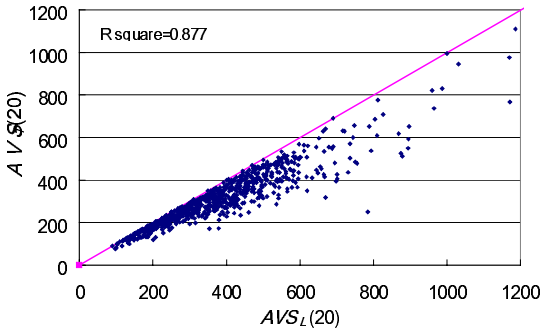

Figure. 3 Comparison between two definitions of average shear wave velocity (*AVS*)

The physical meaning of the *AVS* is investigated by using simplified soil models. The transfer function between a soil surface and a rock outcrop for a 3-layer model (Fig. 4) is obtained as follows based on the wave propagation theory.

$$|H(\omega)| = \frac{1}{\sqrt{\left(\cos\frac{\omega H_1}{V_1}\cos\frac{\omega H_2}{V_2} - \frac{\rho_1 V_1}{\rho_2 V_2}\sin\frac{\omega H_1}{V_1}\sin\frac{\omega H_2}{V_2}\right)^2 + \left(\frac{\rho_2 V_2}{\rho_3 V_3}\cos\frac{\omega H_1}{V_1}\sin\frac{\omega H_2}{V_2} - \frac{\rho_1 V_1}{\rho_3 V_3}\sin\frac{\omega H_1}{V_1}\cos\frac{\omega H_2}{V_2}\right)^2}} \qquad (5)$$

Then the predominant frequency satisfies the following equation:

$$\tan\frac{\omega H_1}{V_1}\tan\frac{\omega H_2}{V_2} = \frac{\rho_1 V_1}{\rho_2 V_2} \qquad (6)$$

in which V_i is the S-wave velocity and H_i is the thickness of the ith layer. In this study, the damping ratio of the soil is defined as zero. The parameter used for this analysis is shown in Table.1. The image of this procedure is shown in Fig. 4. First, the amplification ratio for a three-layer soil model is calculated and the predominant period (T_1) is obtained for the model. A two-layer model that has the same predominant period with the three-layer model is obtained. The parameters for this soil model are given as V_{opt} for the S-wave velocity and H_{opt} for the layer thickness. The relationship between V_{opt}, H_{opt} and T_1 is obtained from Eq. (7). The relationship between the parameters of each model is shown in Eq. (8). From these equations, H_{opt} and V_{opt} is given as

Table 1 Parameters used for the analysis

	Case1	Case2
V_1 (m/s)	200	200
H_1 (m)	10	10
V_2 (m/s)	400	100
H_2 (m)	10	10
V_b (m/s)	600	
T_1 (s)	0.23	0.76
V_{opt} (m/s)	126	227
H_{opt} (m)	13.2	24.0
AVS_{Hopt} (m/s)	126	227

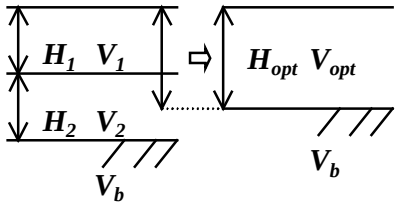

Figure 4 The image of the procedure to identify H_{opt} and V_{opt} of the equivalent two-layer model

$$\frac{T_1}{4} = \frac{H_{opt}}{V_{opt}} \tag{7}$$

$$\frac{H_1}{V_1} + \frac{H_{opt} - H_1}{V_2} = \frac{H_{opt}}{V_{opt}} \tag{8}$$

From Eq.(8), an equation of V_{opt} that describes the definition of $AVS_T(H_{opt})$ is given. Therefore, the meaning to calculate the $AVS_T(H_{opt})$ for a three-layer soil model is to obtain the equivalent two-layer soil model having the same predominant period. The results of the analysis are shown in Figs. 5 and 6, which show the correspondence of the predominant period and in the amplification ratio at the period in the two models.

From this investigation, the physical meaning of $AVS_T(d)$ is explained. The difference of H_{opt} in each site is one of the main factor that causes the variation in the correlation between $AVS_T(d)$ and the amplification ratio. Thus the necessity to combine the relationship with borehole information still exists.

The relationships between the *AVS* and PGA and PGV are investigated. The coefficient of determination is used as an index to describe the degree of fitness to the relationship between the *AVS* and site amplification. Figure 7 shows the change of the correlation with the depth. Table 2 shows the depth which gives the highest correlation. The depth of the highest correlation is deeper for the relationship for the $AVS_T(d)$. The relationships between the *AVS* and PGV show high correlation. From this investigation, efficiency of the *AVS* as an indicator to describe the site amplification is

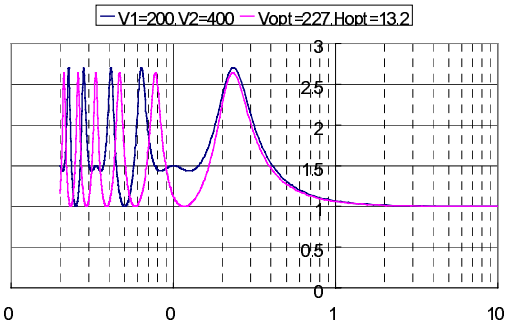

Figure. 5 Transfer function for Case 1

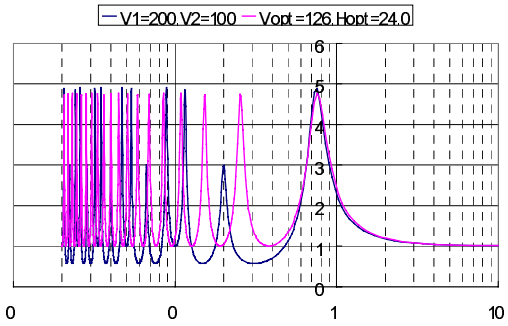

Figure. 6 Transfer function for Case 2

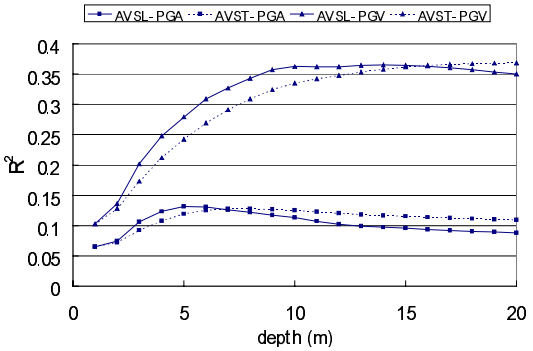

Figure 7 Coefficient of determination as a function of depth

Table 2 The depth which gives the highest correlation

		D(m)	R^2	σ^2
PGA	AVS_L	5	0.132	0.214
	AVS_T	8	0.128	
PGV	AVS_L	14	0.365	0.217
	AVS_T	20	0.368	

confirmed. Figures 8 and 9 show the distribution of the site amplification for the PGV with the *AVS(d)*. The mean relationship between the amplification ratio for *PGV* and *AVS* are obtained as Eqs. (9) and (10).

$$\log_{10}(AR_{PGV})=-0.649*\log_{10}(AVS_L(14))+1.61 \quad (9)$$

$$\log_{10}(AR_{PGV})=-0.734*\log_{10}(AVS_T(20))+1.81 \quad (10)$$

and those for *PGA* and *AVS* are

$$\log_{10}(AR_{PGA})=-0.416*\log_{10}(AVS_L(5))+0.961 \quad (11)$$

$$\log_{10}(AR_{PGA}) =-0.436*\log_{10}(AVS_T(8))+1.0 \quad (12)$$

The relationship between the *AVS* and the site amplification spectra is also investigated. Figures 10 and 11 show the change of the depth with the period that the correlation between the *AVS*

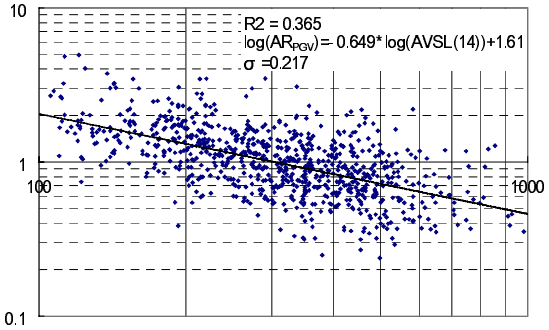

Figure. 8 Distribution of the amplification ratio with $AVS_L(14)$

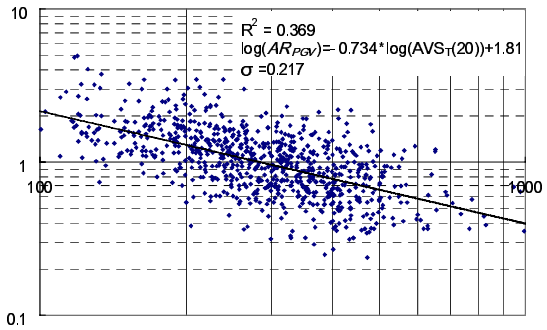

Figure. 9 Distribution of the amplification ratio with $AVS_T(20)$

and site amplification ratios for the acceleration and velocity response spectra becomes the highest. As shown for PGA and PGV, the depth corresponding to the highest correlation in $AVS_T(d)$ is deeper than that of $AVS_L(d)$. Figures 12 and 13 show the relationships between the period and the correlation of the

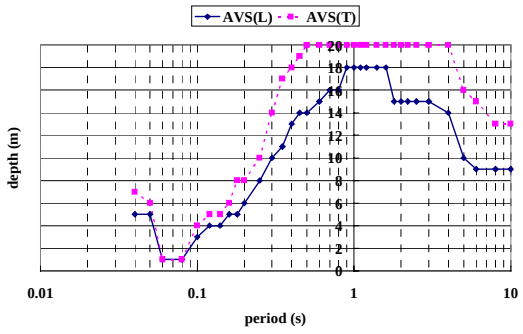

Figure. 10 Depth showing the highest correlation for the acceleration response spectrum

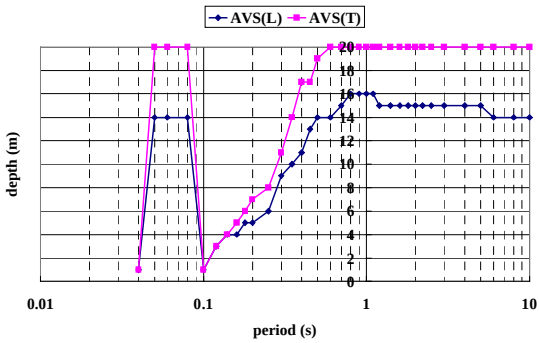

Figure. 11 Depth showing the highest correlation for the velocity response spectrum

$AVS_T(20)$ with the amplification ratio. In the correlation between *AVS* and the amplification of S_A, a period around 0.7s shows the highest correlation. In the amplification of S_V, the correlation is high in the long period range. The K-NET data used in this study do not contain large magnitude events, which have long period contents. It is also pointed out that the soil profiles for K-NET sites are limited to -20m from the ground surface. Thus, further investigations for the relationships between the *AVS* and the site amplification may be necessary.

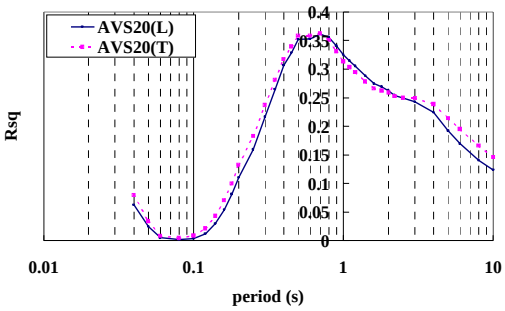

Figure. 12 R^2 for the relationship between *AVS* and the amplification of S_A

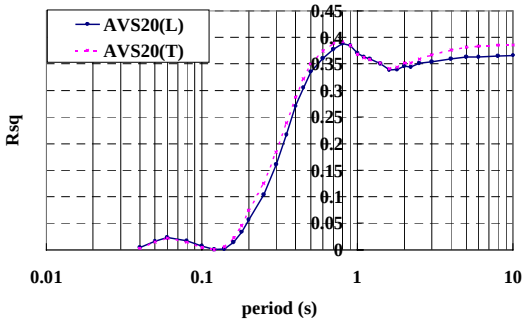

Figure. 13 R^2 for the relationship between *AVS* and the amplification of S_V

Conclusions

The relationships between the average shear wave velocity (*AVS*) and site amplification ratios of the strong motion indices (PGA, PGV) and the response spectrum were investigated. First, the physical meaning of the *AVS* was explained using the transfer function of a two-layer soil model, which simulates a three-layer model. The *AVS* and the depth to calculate *AVS* are highlighted as factors of the equivalent two-layer model. Using the station coefficients in the attenuation relationships for the K-NET records, the *AVS* was found to be an effective indicator to describe the site amplification characteristics. The relationship was also valid for the site amplification of response spectra. Due to the limitation of the data used, a further investigation is necessary to establish more solid conclusions.

References

Fukuwa N, Arakawa M, Nishizaka R. Estimation of site amplification factor using Digital National Land Information. *Journal of Structural Engineering* 1998; 44(B): 77- 84 (in Japanese)

Matsuoka M, Midorikawa S. GIS-based integrated seismic hazard mapping for a large metropolitan area. *Proceeding of the Fifth International Conference on Seismic Zonation* 1995;II 1334- 41

Shabestrai K, Yamazaki F. Attenuation relation spectra in Japan considering site-specific term. *12th WCEE* CD-ROM ref. No. 1432, 2000.

Yamazaki F, Noda S, Meguro K. Developments of early earthquake damage assessment systems in Japan. In: Balkema AA, editor. *Structural safety and reliability, Proceedings of ICOSSAR'97*, 1998. pp. 1573-80

Yamazaki F, Wakamatsu K, Onishi J, and Shabestari K.T. Relationship between geomorphological land classification and site amplification ratio based on JMA strong motion records. *Soil Dynamics and Earthquake Engineering* 2000: 41-53